Environment International 163 (2022) 107214

Contents lists available at ScienceDirect

Environment International

journal homepage: www.elsevier.com/locate/envint

Full length article

An observation-based adjustment method of regional contribution estimation from upwind emissions to downwind $PM_{2.5}$ concentrations

Minah Bae [a], Byeong-Uk Kim [b], Hyun Cheol Kim [c,d], Jung Hun Woo [e], Soontae Kim [f,*]

[a] Department of Environmental Engineering, Ajou University, Suwon 16499, South Korea
[b] Georgia Environmental Protection Division, Atlanta, GA 30354, USA
[c] Air Resources Laboratory, National Oceanic and Atmospheric Administration, College Park, MD 20740, USA
[d] Cooperative Institute for Satellite Earth System Studies, University of Maryland, College Park, MD 20740, USA
[e] Department of Advanced Technology Fusion, Konkuk University, Seoul 05029, South Korea
[f] Department of Environmental and Safety Engineering, Ajou University, Suwon 16499, South Korea

ARTICLE INFO

Handling Editor: Adrian Covaci

Keywords:
$PM_{2.5}$
Long-range transport
Contribution
Adjustment
Northeast Asia

ABSTRACT

We propose a method to adjust contributions from upwind emissions to downwind $PM_{2.5}$ concentrations to account for the differences between observed and simulated $PM_{2.5}$ concentrations in an upwind area. Emissions inventories (EI) typically have a time lag between the inventory year and the release year. In addition, traditional emission control policies and social issues such as the COVID-19 pandemic cause steady or unexpected changes in anthropogenic emissions. These uncertainties could result in overestimation of the emission impacts of upwind areas on downwind areas if emissions used in modeling for the upwind areas were larger than the reality. In this study, South Korea was defined as the downwind area while other regions in Northeast Asia including China were defined as the upwind areas to evaluate applicability of the proposed adjustment method. We estimated the contribution of emissions released from the upwind areas to $PM_{2.5}$ concentrations in South Korea from 2015 to 2020 using a three-dimensional photochemical model with two EIs. In these two simulations for 2015–2020, the annual mean foreign contributions differed by 4.1–5.5 μg/m^3. However, after adjustment, the differences decreased to 0.4–1.1 μg/m^3. The adjusted annual mean foreign contributions were 12.7 and 8.8 μg/m^3 during 2015–2017 and 2018–2020, respectively. Finally, we applied the adjustment method to the COVID-19 pandemic period to evaluate the applicability for short-term episodes. The foreign contribution of $PM_{2.5}$ during the lock-down period in China decreased by 30% after adjustment and the $PM_{2.5}$ normalized mean bias in South Korea improved from 15% to −4%. This result suggests that the upwind contribution adjustment can be used to alleviate the uncertainty of the emissions inventory used in air quality simulations. We believe that the proposed upwind contribution adjustment method can help to correctly understand the contributions of local and upwind emissions to $PM_{2.5}$ concentrations in downwind areas.

1. Introduction

Quantitative source-receptor analysis for a certain area can provide important information for air quality improvement such as pollutant emissions from the area as well as the impacts of those from surrounding areas on $PM_{2.5}$ concentrations in the region of interest (Clappier et al., 2017). In Northeast Asia, such analyses have been conducted with an aim to quantify the long-range transport of air pollutants between regions using three-dimensional photochemical models (e.g., CMAQ, CAMx, and GEOS-Chem) and other tools (Itahashi et al., 2012; Wang et al., 2015; Choi et al., 2019; Bae et al., 2020a; Kumar et al., 2021). According to these studies, air pollutants emitted from China contribute to approximately 40–70% of total $PM_{2.5}$ concentrations in South Korea, a country located downwind of China (Bae et al., 2020a; c; Kumar et al., 2021).

The accuracy of source-receptor analysis results is important in terms of information utilization for development and implementation of State Implementation Plans and population exposure assessment, etc. Accordingly, input data, such as emissions, should accurately reflect the actual status. An emissions inventory, as one of the main inputs for air

* Corresponding author.
E-mail addresses: bma829@ajou.ac.kr (M. Bae), byeonguk.kim@gmail.com (B.-U. Kim), hyun.kim@noaa.gov (H.C. Kim), woojh21@gmail.com (J.H. Woo), soontaekim@ajou.ac.kr (S. Kim).

https://doi.org/10.1016/j.envint.2022.107214
Received 6 January 2022; Received in revised form 13 March 2022; Accepted 24 March 2022
Available online 28 March 2022

quality simulations, is often prepared based on socioeconomic activity data (e.g., traffic volume and fuel consumption) and/or with observed emissions data. Therefore, there is usually a lag of two or more years between the period that the emissions inventory represents and its distribution (Wang et al., 2016b; Bae et al., 2020b). For example, from 2013 to 2017, the SO_2 and NO_x emissions in China reportedly decreased by 59% and 21%, respectively (Zheng et al., 2018; Zhang et al., 2019). However, there is no available emissions inventory data after 2017. Moreover, we can expect substantial changes in emissions for January 2020 due to the COVID-19 pandemic (Huang et al., 2021; Kim et al., 2021c). Nevertheless, these changes cannot be accounted for if existing emissions inventories are used in modeling. If actual emissions trends are not reflected in air quality simulations, simulation results would show discrepancies with respect to the observed concentrations (Bae et al., 2020b). Particularly, the differences between the observed and simulated concentrations in upwind areas can affect uncertainty in the estimated contributions of upwind emissions on the air quality of downwind areas. It also can lead to uncertainties of environmental and health risk assessment.

Previous studies have attempted to use observational data to better utilize the simulation results by considering the uncertainties in air quality simulations. Zhang et al. (2018) and Itahashi et al. (2021) attempted to adjust simulated wet deposition values using the ratio of the observed and simulated precipitation. Bae et al. (2017) attempted to adjust the contributions from various emission sources based on the observed concentrations in a receptor region. These methods, however, did not consider the simulation uncertainty over the upwind area specifically for the downwind areas.

In this study, we propose an approach to adjust modeled contributions of emissions from upwind areas to the $PM_{2.5}$ concentrations in a downwind area. The proposed contribution adjustment approach was designed to address the uncertainty of the simulation results for the upwind area by adjusting upwind emission impacts using ratios of observed $PM_{2.5}$ concentrations to simulated $PM_{2.5}$ concentrations in the upwind area. To evaluate the temporal extent of the applicability of the contribution adjustment approach presented in this study, we conducted not only a long-term analysis from 2015 to 2020 but also a short-term analysis for the COVID-19 pandemic period.

2. Methods and data

2.1. Contribution calculations and adjustment methods

To analyze the contribution of upwind emissions to the $PM_{2.5}$ concentrations in a downwind area, two types of methods can be used with three-dimensional air quality modeling. One is the tagging method that designates a marker for each modeled pollutant from a specific emission area or an emission source during the simulation and tracks the tagged pollutant throughout the physical processes and chemical reactions that the marked pollutant experiences in the model. The other is the brute force method (BFM) that estimates the zero-out contribution (ZOC) by taking the difference between a base run without any emission perturbation and a sensitivity simulation by perturbing the emissions of a target source to a certain level. In this study, we used the BFM as follows. Northeast Asia including China was set as the upwind area (the source), and South Korea was set as the downwind area (the receptor). Westerly or northwesterly winds are prevalent in Northeast Asia (Itahashi et al., 2013; Jeon et al., 2019). Additionally, backward trajectories also show that most of the air masses come from the western side of South Korea (Figure S1). The upwind area contribution (U_ZOC_{Base}) to the downwind area and the relative upwind area contribution (RU_ZOC_{Base}) were calculated as follows:

$$U\_ZOC_{Base} = \left(MOD^{downwind}_{Base} - MOD^{downwind}_{Sens,\Delta E}\right) \times \frac{100\%}{\Delta E(\%)} \quad (1)$$

$$RU\_ZOC_{Base} = \frac{U\_ZOC_{Base}}{MOD^{downwind}_{Base}} \times 100(\%) \quad (2)$$

$$D\_ZOC_{Base} = MOD^{downwind}_{Base} - U\_ZOC_{Base} \quad (3)$$

where $MOD^{downwind}_{Base}$ and $MOD^{downwind}_{Sens,\Delta E}$ denote the modeled concentration from the base run and the modeled concentration in the sensitivity simulation in the downwind area. The sensitivity simulation was performed by reducing the emissions of all pollutants from Northeast Asia, except for South Korea by 50% (i.e., $\Delta E = 50$). For BFM with a 100% reduction in emission, inaccurate (e.g., negative) contributions can be estimated in the vicinity of high emissions sources owing to the numerical error and non-linear chemistry. Koo et al. (2009), Clappier et al. (2017), and Kim et al. (2017b) report that the contributions estimated using BFM with 20%, 50%, and 100% perturbations can be different from each other by up to 10%. In this study, considering the nonlinear relationship between emission-concentration and the recent rate of decrease in the Chinese emission, 38 ~ 60% as reported by Zheng et al. (2018), the reduction rate for the sensitivity run was set at 50%, consistent with Kim et al. (2017b) and Bae et al. (2020c). As defined in Eq. (3), the downwind contribution (D_ZOC_{Base}) was assumed to be the result of subtracting U_ZOC_{Base} from$MOD^{downwind}_{Base}$.

Appreciable discrepancies between the observed and simulated concentrations in upwind areas lead to uncertainty in estimating the impact of upwind area emissions on air quality in a downwind area. In turn, this type of uncertainty prevents accurate accounting for culpability for the air quality status in the receptor region. Therefore, we adjusted the emissions impact from an upwind area to air quality in a downwind area based on the uncertainty of air quality simulation results in the upwind area. We call this method as the "upwind contribution adjustment" and defined the adjustment factor,AF^{upwind}, as follows:

$$AF^{upwind} = OBS^{upwind}/MOD^{upwind}_{Base} \quad (4)$$

where, OBS^{upwind} and MOD^{upwind}_{Base} are the observed concentrations in the upwind area and the simulated concentrations in the upwind area by the base run. Previous studies (Wang et al., 2016a; Choi et al., 2019; LTP, 2019; Yim et al., 2019) have estimated the relative contribution of Japanese emissions to $PM_{2.5}$ concentration in South Korea at less than 2%. Therefore, AF^{upwind} in this study was calculated using the observed and simulated concentrations in China.

WithAF^{upwind}, we estimated adjusted upwind contribution (U_ZOC_{Adj}) and relative adjusted upwind contribution (RU_ZOC_{Adj}) as follows:

$$U\_ZOC_{Adj} = U\_ZOC_{Base} \times AF^{upwind} \quad (5)$$

$$MOD^{downwind}_{Adj} = U\_ZOC_{Adj} + D\_ZOC_{Base} \quad (6)$$

$$RU\_ZOC_{Adj} = \frac{U\_ZOC_{Adj}}{MOD^{downwind}_{Adj}} \times 100(\%) \quad (7)$$

where, $MOD^{downwind}_{Adj}$ denotes the adjusted modeled concentration in the downwind area. By definition, U_ZOC_{Base} and U_ZOC_{Adj} represent foreign contributions before and after adjustment, respectively. Likewise, RU_ZOC_{Base} and RU_ZOC_{Adj} are relative foreign contributions before and after adjustment, respectively. While the relative domestic contributions before and after adjustments, RD_ZOC_{Base} (%) and RD_ZOC_{Adj} (%), respectively were calculated as follows:

$$RD\_ZOC_{Base} = 100 - RU\_ZOC_{Base} \quad (8)$$

$$RD\_ZOC_{Adj} = 100 - RU\_ZOC_{Adj} \quad (9)$$

Fig. 1 shows an example of an upwind contribution adjustment. Although this method cannot directly improve the uncertainty in the emission inventory, it was possible to evaluate the contribution

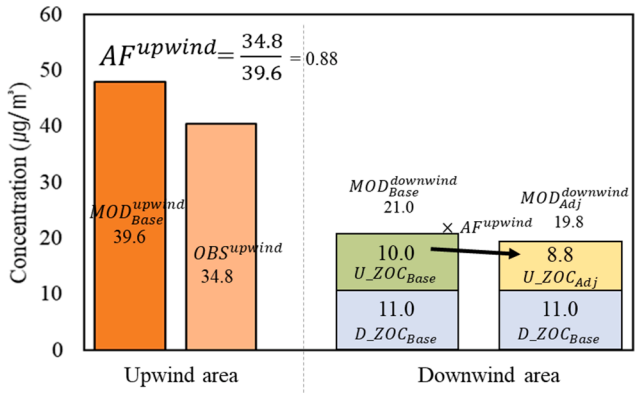

Fig. 1. An illustrative example of how to estimate adjusted upwind contributions in downwind areas. $\mathbf{OBS^{upwind}}$ and $\mathbf{MOD^{upwind}_{Base}}$ refer to the observed concentrations and the modeled $PM_{2.5}$ concentrations by a base simulation in upwind areas, respectively. $\mathbf{AF^{upwind}}$ is an adjustment factor. $\mathbf{MOD^{downwind}_{Base}}$ denotes the $PM_{2.5}$ concentrations with a base simulation in downwind areas. $\mathbf{U\_ZOC_{Base}}$ and $\mathbf{D\_ZOC_{Base}}$ indicate the contributions from the upwind and downwind areas to the downwind areas, respectively. $\mathbf{U\_ZOC_{Adj}}$ is an adjusted value of$\mathbf{U_ZOC_{Base}}$. $\mathbf{MOD^{downwind}_{Adj}}$ is the adjusted $PM_{2.5}$ concentration in the downwind areas.

indirectly by considering the uncertainty in the simulation results. The adjustment method proposed in this study assumed that the simulation uncertainty in the upwind area is primarily caused by the emission uncertainty. However, notably, the uncertainty of the meteorological simulation can also affect the accuracy of the contribution estimate.

2.2. Surface observation data

To evaluate the meteorological simulation results, we compared the simulation results with the observed temperatures and wind speeds from the Meteorological Assimilation Data Ingest System (MADIS) sites in China and South Korea (https://madis.ncep.noaa.gov). The hourly surface $PM_{2.5}$ observation data from China and South Korea were used to evaluate the performance of the air quality simulation and to adjust upwind contributions with Eqs. (4) and (5).

Notably, the number of observational stations for the surface air quality used in this study varied by year since observation stations were newly installed or closed in both China and South Korea. Fig. 2 shows the locations of the observation stations in 2020 and all available data obtained from the observation stations for each year from 2015 to 2020 were used in this study. The total numbers of observational sites for $PM_{2.5}$ in China and South Korea used in this study were 1610 stations maintained by the China National Environmental Monitoring Center (https://www.cnemc.cn/en) and 416 stations of the urban air monitoring network operated by the National Institute of Environmental Research of South Korea (https://www.airkorea.or.kr), respectively.

2.3. Analysis period and input data preparation

The analysis period of this study was from January 1, 2015 to December 31, 2020. For meteorological data for air quality simulations, the Weather Research and Forecasting (WRF; Skamarock et al., 2008) model version 3.9.1 was used. The WRF simulation was performed for 15-day blocks with a one-day pre-run throughout the modeling period. The National Center for Environmental Prediction-Final (NCEP FNL; NCEP, 2000) was used as the initial and boundary meteorological field. Analysis nudging was performed for wind, temperature, and moisture above PBL for 6-hour intervals. WRF results were further processed with the Meteorology-Chemistry Interface Processor (MCIP) version 3.6 to prepare the model-ready meteorological input data for air quality simulations. Anthropogenic emissions were prepared by processing the foreign and domestic emissions inventories with the Sparse Matrix Operator Kernel Emissions (SMOKE; Benjey et al., 2001) version 3.1. Biogenic emissions were prepared with the Model of Emission of Gases and Aerosols from Nature (MEGAN; Guenther, 2006). Air quality simulations were performed using the Community Multiscale Air Quality (CMAQ; Byun and Schere, 2006) version 4.7.1. The CMAQ model was run with SAPRC99 (Carter, 2000) for gas-phase chemical mechanism and AERO5 for aerosol simulations including ISORROPIA for inorganic partitioning and RADM for aqueous-phase chemical reactions. Table 1 summarizes the detailed simulation configurations of the WRF and CMAQ models.

The meteorological and air quality simulation domain for Northeast Asia including China was set at a 27-km horizontal resolution (Fig. 2a). To simulate air quality in South Korea, a finer grid domain was set at a 9-

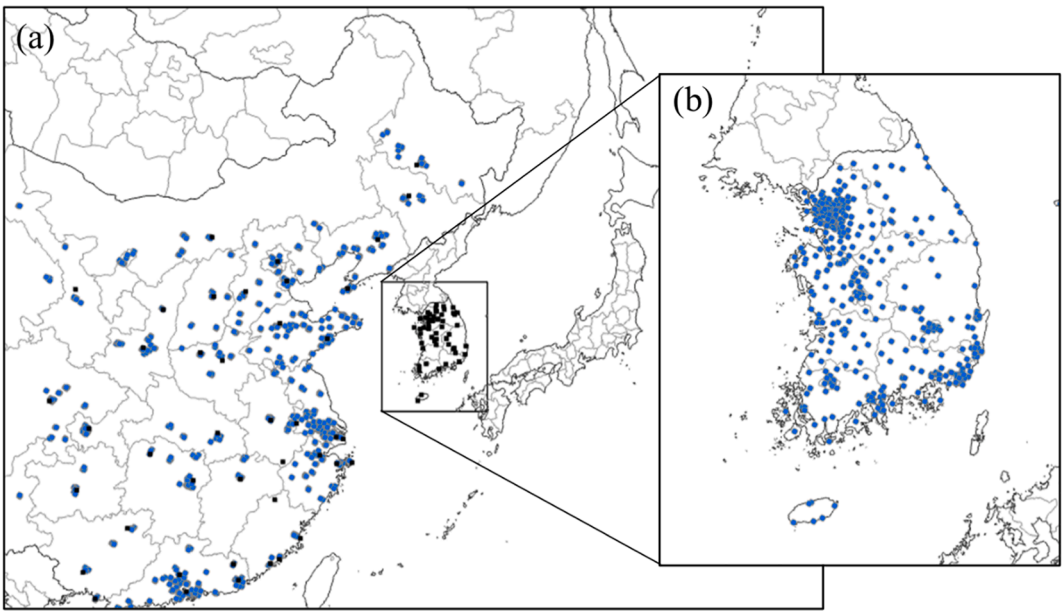

Fig. 2. Modeling domains with (a) 27-km and (b) 9-km horizontal grid resolutions. Black squares and blue circles depict the locations of the Meteorological Assimilation Data Ingest System (MADIS) sites and surface air quality measurement sites, respectively.

Table 1
WRF and CMAQ configurations used in this study.

WRF		CMAQ	
Micro Physics	WSM 6-class	Aerosol Module	AERO5
Cumulus Scheme	Kain-Fritsch	Chemical Mechanism	SAPRAC 99
Long-Wave Radiation	RRTMG	Advection Scheme	YAMO
Short-Wave Radiation	RRTMG	Horizontal Diffusion	Multiscale
PBL Scheme	YSU	Vertical Diffusion	Eddy
		Cloud Scheme	RADM

km horizontal resolution (Fig. 2b). The base and sensitivity simulation results for the 27-km domain were used to extract boundary conditions for the 9-km domain runs to perform the foreign contribution analysis following the approach used by Bae et al. (2020c) (Table 2).

To ensure that the proposed contribution adjustment method was applicable to a broad range of emission scenarios, we performed simulations with more than one emission scenario. Specifically, we evaluated four emissions inventories frequently used for simulating air quality in Northeast Asia and selected two inventories that can represent a range of emission variations in the upwind area: CREATE 2015 (Woo et al., 2020) and KORUSv5 (Woo et al., n.d.). Details about our selection process and results are presented in Section 3.1. For the downwind area, the Clean Air Policy Support System (CAPSS) 2016 emissions inventory was used for all simulations. The CMAQ simulation results using emissions based on CAPSS 2016 and CREATE 2015 were termed "C15" while the CMAQ simulation results using emissions based on CAPSS 2016 and KORUSv5 were termed "Kv5." Therefore, all other input data and simulation configurations were identical between C15 and Kv5 except for the foreign emissions inventories. C15 and Kv5 spanned the entire study period from January 1, 2015 to December 31, 2020.

3. Results

3.1. Comparison of Chinese emissions in existing emissions inventories

In CREATE 2015, MEIC 2017 (Zheng et al., 2018), REASv3 (Kurokawa and Ohara, 2020), and KORUSv5 emissions inventories, the differences between the maximum and minimum emissions of Chinese SO_2 and $PM_{2.5}$ were 160% and 88%, respectively. For other pollutants, the differences between the maximum and minimum emissions ranged from 22% to 37% (Fig. 3). Among these four emissions inventories, CREATE 2015 had the highest emissions while KORUSv5 had the lowest emissions overall. Moreover, these two emissions inventories have been used in various studies for analyses of the air quality in Northeast Asia, including the 2016 KORUS-AQ field campaign (Choi et al., 2019; Crawford et al., 2021; Kim et al., 2021a; b). Thus, we selected these two inventories to reflect the uncertainty range to the greatest possible extent.

The CREATE 2015 emissions were 17% to 105% higher for all substances (excluding VOCs) than the KORUSv5 emissions (Fig. 3). The SO_2 emissions were 27,425 ktons/year (KTPY) in CREATE 2015 and 13,374 KTPY in KORUSv5, 50% less in KORUSv5 than CREATE 2015. VOC emissions were 22,644 KTPY in CREATE 2015 and 28,356 KTPY in KORUSv5. The spatial distributions of pollutant emissions represented in these two inventories were similar: The NOx, SO_2, and $PM_{2.5}$ emissions were mainly emitted in large city areas, such as Beijing-Tianjin-Hebei (BTH) and the Yangtze River Delta (YRD) (Figure S2).

Table 2
Descriptions of a set of air quality simulations performed in this study.

Run	Description
Base	- Simulations with 100% emissions in the 27- and 9-km domains
Sensitivity	- Simulation with 50% reduced emissions for the 27-km domainSimulation for the 9-km domain with the boundary conditions from the 27-km simulation with/without emission perturbations (i.e., base and sensitivity simulations for the 27-km domain).

The inventory years of the four emission inventories were 2015 for CREATE 2015 and REASv3, 2016 for KORUSv5, and 2017 for MEIC, respectively. As pointed out in the Introduction section, there is a time lag of several years between the release of the bottom-up inventories (e.g., 2015 to 2017) and the present time (e.g., 2021). To consider the uncertainty in the emissions inventory and the assessment of air pollutant emissions for recent years, top-down emissions can be estimated based on surface or satellite observations. However, top-down emissions can only be estimated for substances that have available observational data. For $PM_{2.5}$, there is uncertainty in the top-down emissions estimation itself due to the differences in the measurement methods and targets between satellite observation data (i.e., aerosol optical depth) and surface observation data (i.e., $PM_{2.5}$) (Lorente et al., 2017; Bae et al., 2020b; Elguindi et al., 2020).

3.2. Model performance evaluation

To evaluate the results of the meteorological simulation from 2015 to 2020, the observed and simulated meteorological values for China and South Korea were compared at the meteorological observation stations. The mean observed and simulated 2-m temperatures for the modeling period were 15.2 and 14.8 °C, respectively (0.4 °C underestimation and correlation coefficient of 0.98). The daily mean observed 2-m temperature value was high in winter and low in summer, and the meteorological simulation reproduced this seasonal variability (Figure S3). The mean observed and simulated 10-m wind speeds for the simulation period were 2.9 and 3.2 m/s, respectively (overestimation of 0.3 m/s and correlation coefficient of 0.73). Overestimation of surface wind speeds may result in the underestimation of surface-level air pollutant concentrations.

The C15 results were evaluated using observational data of the calendar year 2015 for consistency with the inventory year of CREATE 2015, while the Kv5 results were evaluated with observation data of the calendar year 2016 for consistency with the inventory year for KORUSv5. C15 overestimated the average $PM_{2.5}$ concentration over China in 2015 by 6.3 μg/m^3 (12.0% normalized mean bias; NMB) whereas Kv5 underestimated in 2016 by 8.2 μg/m^3 (–17.1% NMB) (Figure S4 and S5). C15 overestimated the mean SO_2 concentration over China in 2015 by 69.1%. This indicates a significant overestimation of SO_2 emissions in the CREATE 2015 as reported by (Bae et al., 2020b). For South Korea, C15 overestimated the mean $PM_{2.5}$ concentration in 2015 by 1.8 μg/m^3 (7.1% NMB) while Kv5 underestimated in 2016 by 6.0 μg/m^3 (–23.0% NMB) (Figure S6 and S7). Kv5 underestimated the NO_2 concentration in South Korea by 0.1 ppb. The underestimation was more pronounced in spring and winter (Figure S7). This is consistent with what has been reported in previous studies: the CAPSS emissions inventory possibly underestimated the NOx emissions in South Korea (Oak et al., 2019; Kim et al., 2020). Table 3 summarizes the performance evaluation statistics. At six supersites in South Korea, the observed secondary inorganic aerosol (SIA; SO_4^{2-}, NO_3^-, and NH_4^+) concentrations were 10.7 μg/m^3 in 2015 and 9.2 μg/m^3 in 2016, respectively. Moreover, the simulated SIA for C15 and Kv5 were 14.9 μg/m^3 in 2015 and 11.4 μg/m^3 in 2016, respectively. The observed and simulated ratios of SIA and $PM_{2.5}$ were 0.4 and 0.6 in 2015, and 0.4 and 0.7 in 2016, respectively. Both simulations had overestimated the SIA concentrations. This overestimation tendency was most likely due to the overestimation of NO_3^- (Table S1).

3.3. Deviation in modeled annual and monthly mean $PM_{2.5}$ concentrations

The annual mean $PM_{2.5}$ concentration in China was 52.7 μg/m^3 in 2015. Particularly, the annual mean $PM_{2.5}$ concentration in BTH was 67.1 μg/m^3 in 2015. That was 27% higher than that of all the areas over China in 2015. Fig. 4 shows that annual mean $PM_{2.5}$ concentrations in China had steadily decreased since 2015. In 2020, it was less than 60 μg/

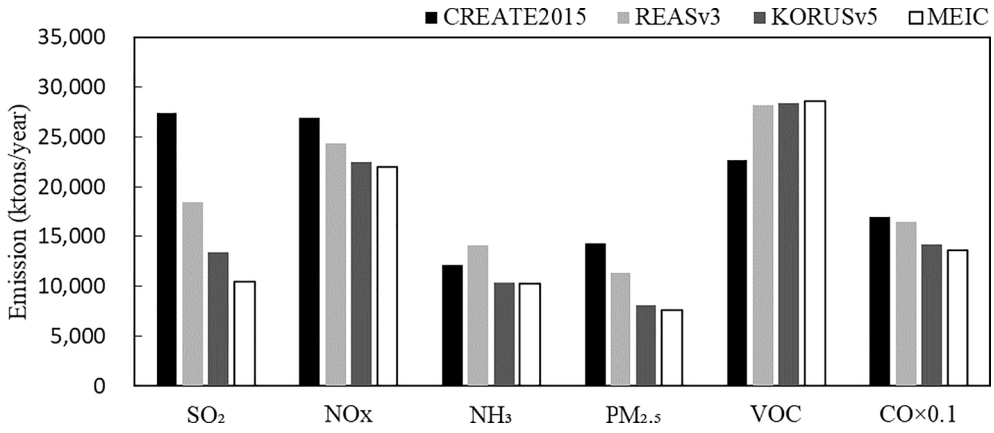

Fig. 3. Comparison of Chinese emissions in the CREATE 2015, REASv3, MEIC, and KORUSv5 emissions inventories. The inventory year of CREATE 2015 and REASv3 is 2015 while the inventory years of KORUSv5 and MEIC are 2016 and 2017, respectively.

Table 3
WRF and CMAQ model performance evaluation over China and South Korea. The modeled 2-m temperatures and 10-m wind speeds were evaluated from 2015 to 2020 while the simulated $PM_{2.5}$ concentrations for C15 and Kv5 were evaluated for 2015 and 2016, respectively.

			Observed mean	Simulated mean	Mean bias	NMB (%)	NME (%)	Correlation coefficient (r)	RMSE
2-m Temperature (°C)			15.1	14.7	−0.4	−2.8	3.7	1.00	0.7
10-m Wind speed (m/s)			2.9	3.2	0.3	10.6	11.6	0.90	0.4
C15	$PM_{2.5}$ (μg/m^3)	China	52.7	59.0	6.3	12.0	18.3	0.90	11.7
		South Korea	25.4	27.2	1.8	7.1	29.4	0.85	10.4
	SO_2 (ppb)	China	9.6	16.3	6.7	69.1	69.1	0.89	7.2
		South Korea	5.1	5.0	−0.1	−1.4	23.6	0.74	1.5
	NO_2 (ppb)	China	16.4	16.1	−0.3	−1.8	12.2	0.83	2.5
		South Korea	23.2	23.2	0.0	0.2	17.3	0.80	4.9
Kv5	$PM_{2.5}$ (μg/m^3)	China	48.0	39.8	−8.2	−17.1	18.6	0.91	12.3
		South Korea	26.0	20.0	−6.0	−23.0	25.5	0.84	8.3
	SO_2 (ppb)	China	8.3	10.3	2.0	24.8	25.9	0.90	2.5
		South Korea	4.6	4.3	−0.3	−7.8	24.2	0.65	1.4
	NO_2 (ppb)	China	16.4	17.9	1.5	9.1	13.8	0.85	2.9
		South Korea	22.6	22.5	−0.1	−0.5	19.3	0.71	5.5

m^3 at all but one observation site in Near Beijing (NRB), and the annual average $PM_{2.5}$ concentration in China was 34.8 μg/m^3 (34% lower than 2015). The $PM_{2.5}$ concentration in BTH was 44.4 μg/m^3 in 2020, and it was a significantly (71%) lower than 2015.

In contrast, the annual mean $PM_{2.5}$ concentration of C15 in China decreased only by 6% (3.5 μg/m^3) from 59.3 to 55.8 μg/m^3 during 2015–2020. This led to steady increases in annual $PM_{2.5}$ deviations between the observation and C15 from 6.6 μg/m^3 (13% NMB) in 2015 to 21.0 μg/m^3 (60% NMB) by 2020. The annual $PM_{2.5}$ concentration of Kv5 over China decreased by 2.4 μg/m^3 from 42.0 to 39.6 μg/m^3 over six years, while the relative decrease rate of 6% was equal to that of C15. However, C15 and Kv5 showed very different biases when compared with the $PM_{2.5}$ observations. Kv5 underestimated the $PM_{2.5}$ concentration by 10.7 μg/m^3 (–20% NMB) in 2015 but began to overestimate the $PM_{2.5}$ concentration in 2019. Then, Kv5 further overestimated the $PM_{2.5}$ concentration by 4.8 μg/m^3 (14% NMB) in 2020. The described deviation trend by C15 and Kv5 over six years shows two noteworthy results. First, air quality simulations using fixed emissions inventories had a limitation in reproducing the decreasing $PM_{2.5}$ concentration trend in China. Second, the selection of an emissions inventory for an air quality simulation can be a major factor that determines the direction of biases in modeled concentrations and, in turn, influences the estimated impacts of upwind emission sources on the air quality in downwind areas. Simulation results may differ with the application of higher horizontal resolution grids (Cohan et al., 2006). High-resolution simulation can potentially reduce differences between observed and simulated $PM_{2.5}$ concentrations (Tan et al., 2015; Bae et al., 2020c). However, in this study, the $PM_{2.5}$ concentrations for China were obtained from simulations with a 27-km horizontal resolution because of computing limitations.

In South Korea, the annual mean observed $PM_{2.5}$ concentration decreased by 26% (from 25.4 to 18.9 μg/m^3) during 2015–2020. For the same period, C15 overestimated the annual mean $PM_{2.5}$ concentration in South Korea in the range of 1.4 to 6.3 μg/m^3 (5% to 33% NMB). Kv5 underestimated the annual mean $PM_{2.5}$ concentration in South Korea by 5.1 μg/m^3 (–12% NMB) in 2015 but showed gradual decreases in overestimation. In 2020, Kv5 only overestimated the annual mean $PM_{2.5}$ concentration by 0.2 μg/m^3 (1% NMB). Notably, while the emission differences between the two simulations were relatively large, the differences in simulated $PM_{2.5}$ concentrations were 30% and 25% in China and South Korea, respectively. This was because $PM_{2.5}$ concentrations included both primary $PM_{2.5}$ directly emitted from the sources and secondary $PM_{2.5}$ through chemical reactions of gaseous precursors in the atmosphere.

As described above, the observed $PM_{2.5}$ concentrations decreased by 34% and 26% from 2015 to 2020 in China and South Korea, respectively. The reduction rates for the simulated $PM_{2.5}$ concentrations in C15 and Kv5 over this period were the same for both China and South Korea at 6% and 13%, respectively. Notably, the reduction rates for the simulated $PM_{2.5}$ concentrations in C15 and Kv5 from 2015 to 2020 were due to the meteorological factors as we performed our simulations consistent with those of previous studies that investigate the

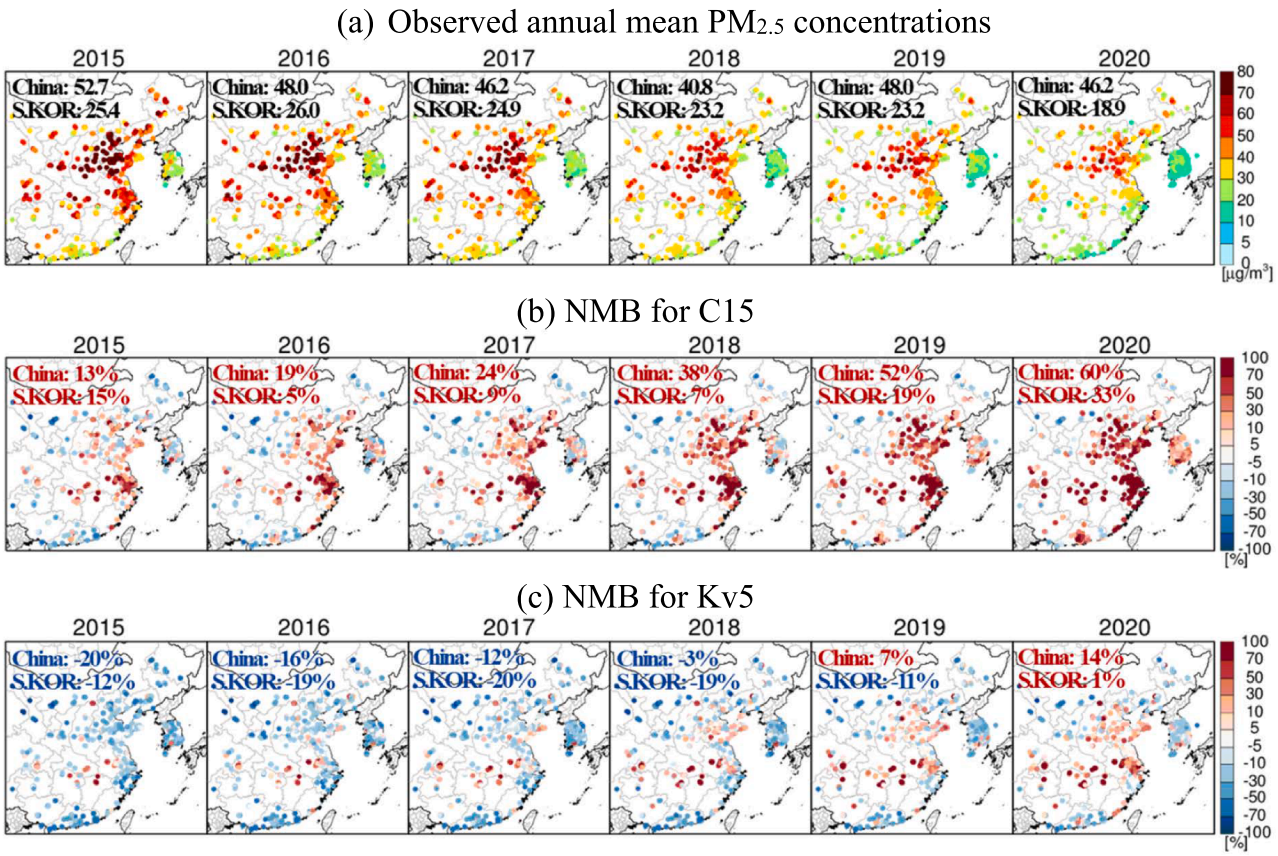

Fig. 4. Spatial distributions of the (a) annual average observed $PM_{2.5}$ concentrations, (b) normalized mean bias (NMB) for C15, and (c) NMB for Kv5 from 2015 to 2020. The mean values over China and South Korea are denoted by letters for each panel. Red and blue letters in (b) and (c) emphasize positive and negative values, respectively.

meteorological effects on air quality trends (Zhang et al., 2019; Bae et al., 2021). Wei et al. (2017), Zhang et al. (2019), and Bae et al. (2021) also report that, recently, meteorological conditions contribute to decreases in $PM_{2.5}$ concentrations over China and South Korea. In general, wind speeds and $PM_{2.5}$ concentrations are negatively correlated. Additionally, precipitation can reduce ambient $PM_{2.5}$ concentrations via wet deposition (Kim et al., 2017a; Chen et al., 2020). In South Korea, the easterly winds often cause an inflow of relatively clean air from the East Sea. We estimated the meteorological factors accounted for 18% (=6/34 × 100) and 50% (=13/26 × 100) of the decrease in the observed $PM_{2.5}$ concentrations over the past six years in China and South Korea. Subsequently, the effects of emission reductions were estimated as 82% (=100 – 18) and 50% (=100 – 50) for China and South Korea, respectively. We noted that the 50% $PM_{2.5}$ concentration reduction in South Korea includes the effect of emission changes in the upwind areas. At the same time, the decrease in the $PM_{2.5}$ concentrations in the upwind areas are likely due to their own emission reductions and those were not small. Therefore, it is important to evaluate the impacts of emission reductions on $PM_{2.5}$ concentrations in South Korea by separating contributions from upwind emissions from the overall contribution to assess the net effects of emission reductions in South Korea. In order to separate the impacts of respective emission reductions in China and South Korea, it was necessary to estimate these through more air quality simulations and analyses. However, it was difficult to quantitatively assess the individual contributions because of the complex nature of chemical reactions as well as the dependency of modeled $PM_{2.5}$ concentrations on meteorology, foreign emissions, and domestic emissions. Further investigations are needed to separate the impacts of foreign and domestic emissions on South Korea.

3.4. Upwind $PM_{2.5}$ contribution

The range of annual mean $U\_ZOC_{Base,C15}$ was estimated to be 13.7–15.9 μg/m^3 and $U\_ZOC_{Base,Kv5}$ was 8.5–10.7 μg/m^3 (Fig. 5a) during 2015–2020. The range of annual mean $U\_ZOC_{Adj,C15}$ was 8.6–14.1 μg/m^3 during 2015–2020. The range of differences between $U\_ZOC_{Base,C15}$ and $U\_ZOC_{Base,Kv5}$ was 4.1–5.5 μg/m^3 (36–55%). However, after adjustment, the differences of $U\_ZOC_{Adj,C15}$ and $U\_ZOC_{Adj,Kv5}$ decreased to 0.4–1.1 μg/m^3 (4–9%). These results suggest that similar foreign contributions can be estimated if the upwind contribution adjustment is made with the proposed adjustment approach in this study regardless the difference in emissions in the upwind area.

Since the annual $U\_ZOC_{Adj,C15}$ and $U\_ZOC_{Adj,Kv5}$ were similar, we describe the evolution of adjusted foreign contributions over time with$U_ZOC_{Adj,Kv5}$. In 2015, the $U\_ZOC_{Adj,Kv5}$ was 13.5 μg/m^3. Then, the $U\_ZOC_{Adj,Kv5}$ decreased to 11.9 and 11.6 μg/m^3 in 2016 and 2017, respectively. Thereafter, from 2018 to 2020, the $U\_ZOC_{Adj,Kv5}$ decreased to less than 9.0 μg/m^3. Particularly, the $U\_ZOC_{Adj,Kv5}$ in 2020 became the lowest during the study period. As various studies have reported, in 2020, anthropogenic emissions and $PM_{2.5}$ concentrations decreased due to the COVID-19 pandemic (Kang et al., 2020; Huang et al., 2021; Kim et al., 2021c). If the entire analysis period was divided into two periods: 2015 to 2017 (P1) and 2018 to 2020 (P2), the average $U\_ZOC_{Adj,Kv5}$ was lower by 31% (3.8 μg/m^3) during P2 compared with P1.

The $PM_{2.5}$ concentrations in South Korea are relatively high in spring and winter but relatively low in summer (Bae et al., 2020a; Kumar et al., 2021). The seasonal mean $U\_ZOC_{Base,Kv5}$ was highest in winter (13.6 μg/m^3), followed by spring (13.2 μg/m^3), autumn (7.5 μg/m^3), and summer (4.5 μg/m^3) (Fig. 6). The seasonal mean $U\_ZOC_{Adj,Kv5}$ increased by 0.2–1.2 μg/m^3. The order of seasonal mean foreign contributions is

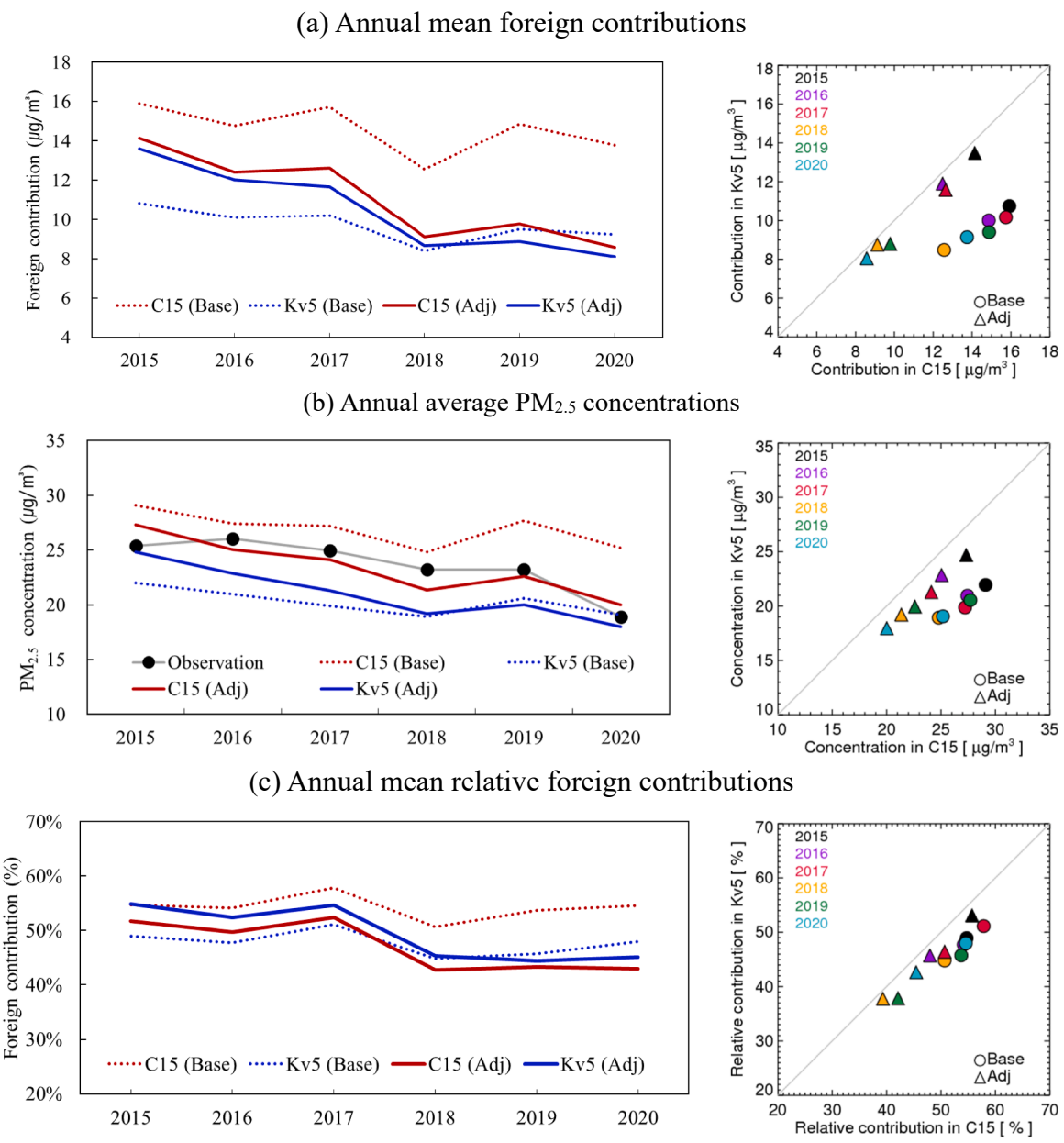

Fig. 5. Time-series and scatter plots for (a) the annual mean foreign contributions to annual average $PM_{2.5}$ concentrations, (b) annual average $PM_{2.5}$ concentrations, and (c) relative foreign contributions to annual average $PM_{2.5}$ concentrations in South Korea from 2015 to 2020 with and without adjustments in modeling results in C15 and Kv5. "Base" indicates modeling results in C15 and Kv5 without adjustment. "Adj" indicates modeling results with adjustment. Black dots and gray lines represent the observed $PM_{2.5}$ concentrations.

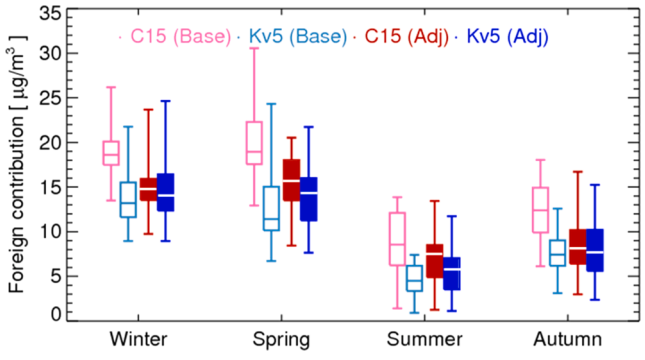

Fig. 6. Seasonal variations in the foreign contributions to $PM_{2.5}$ in South Korea from 2015 to 2020 before and after adjustment.

consistent with that without adjustment, and the same is true for C15. Changes in $U\_ZOC_{Adj,C15}$ and $U\_ZOC_{Adj,Kv5}$ were most prominent in the spring, 4.8 and –1.2 μg/m^3, respectively. In general, spring had high foreign contributions (Bae et al., 2020a; Kumar et al., 2021) since estimated foreign contributions in spring are significantly affected by the uncertainty in the upwind simulation. Overall, the seasonal mean foreign contributions in Kv5 and C15 showed a difference of 3.7–6.4 μg/m^3 before adjustment but the difference reduced to 0.4–1.7 μg/m^3 after adjustment.

3.5. $PM_{2.5}$ concentration in downwind area and foreign contributions

The range of annual $PM_{2.5}$ concentration deviations between the observed values and C15 for South Korea during the study period improved from 1.4 to 6.3 μg/m^3 (before adjustment) to –1.8–1.9 μg/m^3

(after adjustment), as shown in Fig. 5(b). From 2015 to 2018, the range of annual $PM_{2.5}$ concentration deviations between the observation and Kv5 for South Korea was between –5.0 and –3.4 μg/m^3 before adjustment and decreased to –4.0 to –0.6 μg/m^3 after adjustment. From 2019 to 2020, this deviation of Kv5 slightly increased from –2.6 and 0.2 μg/m^3 before adjustment to –3.2 and –0.9 μg/m^3 after adjustment. The annual mean $PM_{2.5}$ concentrations of C15 in South Korea were 5.9–7.3 μg/m^3 higher than those of Kv5 before adjustment. However, after adjustment, the differences were reduced to less than 2.8 μg/m^3. Although by the two simulations the foreign contributions estimated were similar to each other after adjustment, the $PM_{2.5}$ concentrations in South Korea still showed a difference of approximately 2.0 μg/m^3. The differences in the domestic contributions estimated by the two simulations were 1.6–2.0 μg/m^3, which could be attributed to indirect effects (i.e., gaseous precursors or HNO_3 converted to NO_3^-) after migration of $PM_{2.5}$ precursors from the upwind to the downwind area as well as the direct effects of upwind $PM_{2.5}$ depending on the level of emissions in the upwind areas (Chen et al., 2014; Uno et al., 2020; Kim et al., 2021b). In addition, the detailed horizontal and vertical distributions of the emissions used in the two simulations could yield differences. In contrast, both simulations underestimated the $PM_{2.5}$ concentrations in South Korea after the adjustment of the upwind contributions, possibly resulting from an underestimation of the emissions in the downwind area. Accordingly, the relative foreign contribution may be lower than the value estimated in this study.

Before adjustment, the relative foreign contributions (RU_ZOC_{Base}) were 51–58% for C15 and 45–51% for Kv5 during 2015–2020 (Fig. 5c). After adjustment, the relative foreign contributions (RU_ZOC_{Adj}) were 43–52% for C15 and 44–55% for Kv5. The differences in the relative foreign contributions by the two simulations were 5–8% before the adjustment but decreased to less than 3% after adjustment. After accounting for the adjustments to results of C15 and Kv5, the relative foreign contributions decreased by 9% in 2018 as compared to 2015 while the differences between 2019 and 2020 were less than 1%. The adjusted relative domestic contributions (RD_ZOC_{Adj}) were 48–57% for C15 and 45–56% for Kv5.

3.6. Short-term contribution adjustments: Adjustment of daily mean contribution during the COVID-19 pandemic

With a surge in confirmed COVID-19 cases in China at the beginning of 2020, a lockdown was implemented to restrict movement between regions on January 23, 2020. Huang et al. (2021) and Kim et al. (2021c) estimated that NO_x emissions in China decreased by more than 50% due to COVID-19 restrictions. Kang et al. (2020) also reported that 16% and 21% of the $PM_{2.5}$ concentrations decreased during lockdown in China and South Korea, respectively, because of emissions reductions. However, the existing bottom-up emissions inventories are not able to consider these drastic emissions changes. Therefore, we attempted to perform daily upwind contribution adjustments from December 2019 to March 2020 as well as evaluated applicability of our proposed adjustment approach to short-term cases. The analysis period was divided into before and after the implementation of lockdown (January 23, 2020). The analysis results presented below are based on Kv5 only because no significant difference was observed when the same analysis was performed on the C15 results.

The daily average $PM_{2.5}$ concentrations in China before and during lockdown was 65.0 and 42.4 μg/m^3, respectively (Fig. 7). The deviation of $PM_{2.5}$ concentrations between the observation and Kv5 in China increased from 2.5 μg/m^3 (4% NMB) to 14.9 μg/m^3 (35% NMB) when compared before and during the lockdown. In contrast, the observed $PM_{2.5}$ concentrations in South Korea was 27.2 and 22.6 μg/m^3 before and after the beginning of lockdown, respectively. The deviation of $PM_{2.5}$ concentrations between the observation and Kv5 increased from –0.8 μg/m^3 (–3.0% NMB) to 3.5 μg/m^3 (15% NMB) when compared between before lockdown and during the lockdown. The increase in the

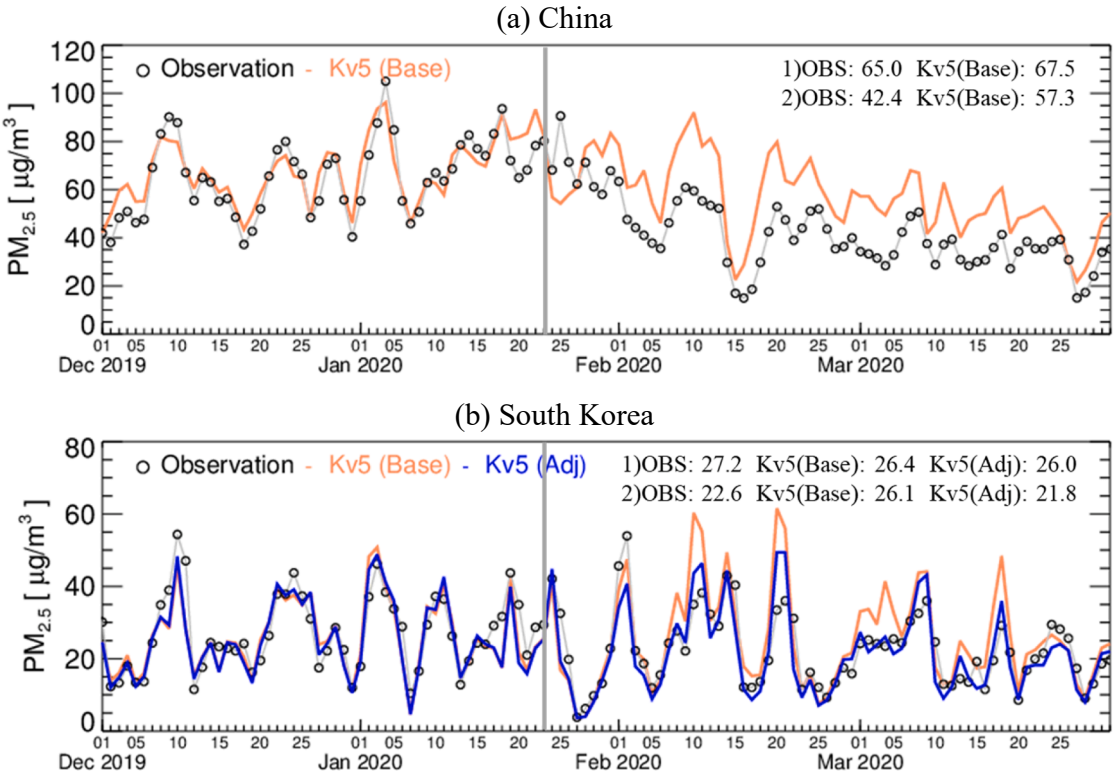

Fig. 7. Observed and simulated daily $PM_{2.5}$ concentrations before and after adjustment from December 2019 to March 2020: (a) China and (b) South Korea. The gray line indicates the beginning of lockdown in China. "1)" and "2)" in the legend indicate the mean $PM_{2.5}$ concentrations in China and South Korea before and during lockdown.

deviation during the lockdown must be due to the reduction in air pollutant emissions from China that were not reflected in the existing emissions inventories as described above. Since South Korea didn't have the lockdown policy implemented for the same period, the aforementioned discrepancies of $PM_{2.5}$ concentrations in China likely propagated into South Korea.

During the lockdown, the $U\_ZOC_{Base,Kv5}$ was 14.3 μg/m^3 (55%) and $U\_ZOC_{Adj,Kv5}$ was 10.1 μg/m^3 (46%). As the foreign contribution decreased by 4.2 μg/m^3 with adjustment, the NMB of Kv5 for $PM_{2.5}$ concentrations in South Korea improved from 15% to –4% during the lockdown. The results of this study suggest that the upwind contribution adjustment method proposed in this study can assess contributions accurately by improving the estimated concentrations in the upwind area even for a short-term episode when abrupt changes in the upwind emissions conditions occur. The number of confirmed COVID-19 cases in South Korea began to increase from the end of March 2020. Therefore, we believe that the effect of the COVID-19 pandemic on the reduction of South Korean emissions was not significant for the modeling period in this study.

4. Conclusions

In this study, we proposed an upwind contribution adjustment method to consider air quality simulation uncertainties in the upwind area (e.g., China) and applied the method to estimate the foreign contribution to the $PM_{2.5}$ concentrations in the downwind area (e.g., South Korea) from 2015 to 2020. While the observed annual mean $PM_{2.5}$ concentrations in China decreased by 34% over the past six years, the air quality simulations (i.e., C15 and Kv5) without considering annual emission changes showed only a 6% decrease. This indicates that air quality simulations with the existing emissions inventories are not sufficient to reflect rapid changes in the $PM_{2.5}$ concentrations in China.

From 2015 to 2020, the annual foreign contributions in C15 to the $PM_{2.5}$ concentrations in South Korea were 13.7–15.9 μg/m^3 (51–58%) before adjustment while those contributions decreased to 8.6–14.1 μg/m^3 (43–52%) after adjustment. In Kv5, the annual foreign contributions were 8.5–10.7 μg/m^3 (45–51%) before adjustment but changed to 8.0–13.5 μg/m^3 (44–55%) after adjustment for the same period. The mean adjusted foreign contribution from 2018 to 2020 decreased by more than 30% compared to that from 2015 to 2017, which indicates that the foreign contributions to the downwind area have declined. Foreign contributions between C15 and Kv5 before adjustment differed by 4.1–5.5 μg/m^3. However, such differences decreased to 0.4–1.1 μg/m^3 after adjustment. This suggests that foreign contributions can be evaluated consistently through the proposed upwind contribution adjustment even though simulated upwind concentration levels are different between C15 and Kv5.

Moreover, the result of applying upwind contribution adjustments for a short-term case (i.e., COVID-19 pandemic) demonstrated that the mean $PM_{2.5}$ concentration deviation between the observation and simulations (i.e., Kv5 and C15) in South Korea improved from 16% to –4% during the lockdown. However, even after adjusting the upwind contributions, the $PM_{2.5}$ concentrations of C15 and Kv5 in South Korea were underestimated. This suggested that air pollutant emissions from South Korea were more likely underestimated. Therefore, the actual domestic contributions would be higher than the estimated contributions. Subsequently, we speculated that the relative foreign contributions, in reality, are lower than the values estimated in this study.

According to the results of this study, the proposed method for upwind contribution adjustment helps to reduce the $PM_{2.5}$ concentration deviation between observation and simulation over both short- and long-term scales and to interpret the impacts of emission reductions on air quality trends accurately. Although we estimated the foreign contributions using the BFM, which is a relatively simple simulation method, the upwind contribution adjustment proposed in this study can be universally applied as the input is independent of the analytical tool or method except for the following caveats. The upwind contribution adjustment approach proposed in this study considered non-linear changes between the emissions and concentrations partially based on the modeled source-receptor relationship under a given emission condition. However, the adjustment approach does not directly account for the uncertainty related to secondary $PM_{2.5}$ formation occurring during the long-range transport of air pollutants from the upwind to the downwind areas.

Funding

This work was supported by Korea Ministry of Environment (KMOE) as Graduate School specialized in Climate Change. This work also supported by KMOE's air pollutants and health project.

CRediT authorship contribution statement

Minah Bae: Investigation, Visualization, Writing – original draft. **Byeong-Uk Kim:** Methodology, Writing – review & editing. **Hyun Cheol Kim:** Software, Writing – review & editing. **Jung Hun Woo:** Resources. **Soontae Kim:** Conceptualization, Writing – review & editing, Supervision.

Declaration of Competing Interest

The authors declare that they have no known competing financial interests or personal relationships that could have appeared to influence the work reported in this paper.

Appendix A. Supplementary material

Supplementary data to this article can be found online at https://doi.org/10.1016/j.envint.2022.107214.

References

Bae, C., Yoo, C., Kim, B.-U., Kim, H.C., Kim, S., 2017. PM2.5 Simulations for the Seoul metropolitan area: (III) Application of the Modeled and Observed PM2.5 Ratio on the Contribution Estimation. Journal of Korean Society for Atmospheric Environment 33 (5), 445–457. https://doi.org/10.5572/KOSAE.2017.33.5.445.

Bae, C., Kim, B.-U., Kim, H.C., Yoo, C., Kim, S. 2020a. Long-range transport influence on key chemical components of PM2.5 in the Seoul metropolitan area, South Korea, during the years 2012–2016, Atmosphere,11(1),48. Multidisciplinary Digital Publishing Institute. doi: 10.3390/atmos11010048.

Bae, C., Kim, H.C., Kim, B.-U., Kim, Y., Woo, J.-H., Kim, S., 2020b. Updating Chinese SO2 emissions with surface observations for regional air-quality modeling over East Asia. Atmos. Environ. 228, 117416. https://doi.org/10.1016/j.atmosenv.2020.117416.

Bae, M., Kim, B.-U., Kim, H.C., Kim, S., 2020. A Multiscale Tiered Approach to Quantify Contributions: A Case Study of PM2.5 in South Korea During 2010–2017. Atmosphere 11 (2), 141. https://doi.org/10.3390/atmos11020141.

Bae, M., Kim, B.-U., Kim, H.C., Kim, J., Kim, S. 2021. Role of emissions and meteorology in the recent PM2.5 changes in China and South Korea from 2015 to 2018, Environmental Pollution, 270116233. doi: 10.1016/j.envpol.2020.116233.

Benjey, W., Houyoux, M., Susick, J. 2001. Implementation of the SMOKE emission data processor and SMOKE tool input data processor in models-3, US EPA.

Byun, D., Schere, K.L., 2006. Review of the governing equations, computational algorithms, and other components of the models-3 community multiscale air quality (CMAQ) modeling system. Appl. Mech. Rev. 59 (2), 51–77. https://doi.org/10.1115/1.2128636.

Carter, W.P.L. 2000. Documentation of the SAPRC-99 Chemical Mechanism for VOC Reactivity Assessment.

Chen, T.-F., Chang, K.-H., Tsai, C.-Y., 2014. Modeling direct and indirect effect of long range transport on atmospheric PM2.5 levels. Atmos. Environ. 891–899. https://doi.org/10.1016/j.atmosenv.2014.01.065.

Chen, Z., Chen, D., Zhao, C., Kwan, M., Cai, J., Zhuang, Y., Zhao, B., Wang, X., Chen, B., Yang, J., Li, R., He, B., Gao, B., Wang, K., Xu, B. 2020. Influence of meteorological conditions on PM2.5 concentrations across China: A review of methodology and mechanism, Environment International, 139105558. 10.1016/j.envint.2020.105558.

Choi, J., Park, R.J., Lee, H.-M., Lee, S., Jo, D.S., Jeong, J.I., Henze, D.K., Woo, J.-H., Ban, S.-J., Lee, M.-D., Lim, C.-S., Park, M.-K., Shin, H.J., Cho, S., Peterson, D., Song, C.-K., 2019. Impacts of local vs. trans-boundary emissions from different sectors on PM2.5 exposure in South Korea during the KORUS-AQ campaign. Atmos. Environ. 203196–203205. https://doi.org/10.1016/j.atmosenv.2019.02.008.

Clappier, A., Belis, C.A., Pernigotti, D., Thunis, P., 2017. Source apportionment and sensitivity analysis: two methodologies with two different purposes. Geosci. Model Dev. 12 https://doi.org/10.5194/gmd-10-4245-2017.

Cohan, D.S., Hu, Y., Russell, A.G., 2006. Dependence of ozone sensitivity analysis on grid resolution. Atmos. Environ. 40 (1), 126–135. https://doi.org/10.1016/j.atmosenv.2005.09.031.

Crawford, J.H., Ahn, J.-Y., Al-Saadi, J., Chang, L., Emmons, L.K., Kim, J., Lee, G., Park, J.-H., Park, R.J., Woo, J.H., Song, C.-K., Hong, J.-H., Hong, Y.-D., Lefer, B.L., Lee, M., Lee, T., Kim, S., Min, K.-E., Yum, S.S., Shin, H.J., Kim, Y.-W., Choi, J.-S., Park, J.-S., Szykman, J.J., Long, R.W., Jordan, C.E., Simpson, I.J., Fried, A., Dibb, J. E., Cho, S., Kim, Y.P., 2021. The Korea-United States Air Quality (KORUS-AQ) field study. Elem. Sci. Anth. 9 (1), 00163. https://doi.org/10.1525/elementa.2020.00163.

Elguindi, N., Granier, C., Stavrakou, T., Darras, S., Bauwens, M., Cao, H., Chen, C., Denier van der Gon, H.A.C., Dubovik, O., Fu, T.M., Henze, D.K., Jiang, Z., Keita, S., Kuenen, J.J.P., Kurokawa, J., Liousse, C., Miyazaki, K., Müller, J.-F., Qu, Z., Solmon, F., Zheng, B., 2020. Intercomparison of Magnitudes and Trends in Anthropogenic Surface Emissions From Bottom-Up Inventories, Top-Down Estimates, and Emission Scenarios, Earth's. Future 8 (8). https://doi.org/10.1029/2020EF001520.

Guenther, A., Karl, T., Harley, P., Wiedinmyer, C., Palmer, P.I., Geron, C., 2006. Estimates of global terrestrial isoprene emissions using MEGAN (Model of Emissions of Gases and Aerosols from Nature). Atmos. Chem. Phys. 6 (11), 3181–3210.

Huang, X., Ding, A., Gao, J., Zheng, B., Zhou, D., Qi, X., Tang, R., Wang, J., Ren, C., Nie, W., Chi, X., Xu, Z., Chen, L., Li, Y., Che, F., Pang, N., Wang, H., Tong, D., Qin, W., Cheng, W., Liu, W., Fu, Q., Liu, B., Chai, F., Davis, S.J., Zhang, Q., He, K., 2021. Enhanced secondary pollution offset reduction of primary emissions during COVID-19 lockdown in China. Natl. Sci. Rev. 8 https://doi.org/10.1093/nsr/nwaa137.

Itahashi, S., Uno, I., Kim, S., 2012. Source Contributions of Sulfate Aerosol over East Asia Estimated by CMAQ-DDM. Environ. Sci. Technol. 46 (12), 6733–6741. https://doi.org/10.1021/es300887w.

Itahashi, S., Uno, I., Kim, S., 2013. Seasonal source contributions of tropospheric ozone over East Asia based on CMAQ–HDDM. Atmos. Environ. 70204–70217. https://doi.org/10.1016/j.atmosenv.2013.01.026.

Itahashi, S., Ge, B., Sato, K., Wang, Z., Kurokawa, J., Tan, J., Huang, K., Fu, J.S., Wang, X., Yamaji, K., Nagashima, T., Li, J., Kajino, M., Carmichael, G.R., Wang, Z., 2021. Insights into seasonal variation of wet deposition over southeast Asia via precipitation adjustment from the findings of MICS-Asia III. Atmos. Chem. Phys. 21 (11), 8709–8734. https://doi.org/10.5194/acp-21-8709-2021.

Jeon, W., Lee, H.W., Lee, T.-J., Yoo, J.-W., Mun, J., Lee, S.-H., Choi, Y., 2019. Impact of varying wind patterns on PM10 concentrations in the Seoul metropolitan area in South Korea from 2012 to 2016. Journal of Applied Meteorology and Climatology 58 (12), 2743–2754. https://doi.org/10.1175/JAMC-D-19-0102.1.

Kang, Y.-H., You, S., Bae, M., Kim, E., Son, K., Bae, C., Kim, Y., Kim, B.-U., Kim, H.C., Kim, S., 2020. The impacts of COVID-19, meteorology, and emission control policies on PM2.5 drops in Northeast Asia. Sci. Rep. 10 (1), 22112. https://doi.org/10.1038/s41598-020-79088-2.

Kim, B.-U., Kim, H.C., Kim, S., 2021a. Effects of vertical turbulent diffusivity on regional PM2.5 and O3 source contributions. Atmos. Environ. 245, 118026. https://doi.org/10.1016/j.atmosenv.2020.118026.

Kim, E., Kim, B.-U., Kim, H.C., Kim, S., 2021b. Direct and cross impacts of upwind emission control on downwind PM2.5 under various NH3 conditions in Northeast Asia. Environ. Pollut. 268, 115794. https://doi.org/10.1016/j.envpol.2020.115794.

Kim, H.C., Kim, S., Kim, B.-U., Jin, C.-S., Hong, S., Park, R., Son, S.-W., Bae, C., Bae, M., Song, C.-K., Stein, A., 2017a. Recent increase of surface particulate matter concentrations in the Seoul Metropolitan Area, Korea. Sci. Rep. 7 (1) https://doi.org/10.1038/s41598-017-05092-8.

Kim, H.C., Kim, E., Bae, C., Cho, J.H., Kim, B.-U., Kim, S., 2017b. Regional contributions to particulate matter concentration in the Seoul metropolitan area, South Korea: seasonal variation and sensitivity to meteorology and emissions inventory. Atmos. Chem. Phys. 17 (17), 10315–10332. https://doi.org/10.5194/acp-17-10315-2017.

Kim, H.C., Kim, S., Lee, S.-H., Kim, B.-U., Lee, P., 2020. Fine-Scale Columnar and Surface NOx Concentrations over South Korea: Comparison of Surface Monitors. TROPOMI, CMAQ and CAPSS Inventory, Atmosphere 11 (1), 101. https://doi.org/10.3390/atmos11010101.

Kim, H.C., Kim, S., Cohen, M., Bae, C., Lee, D., Saylor, R., Bae, M., Kim, E., Kim, B.-U., Yoon, J.-H., Stein, A., 2021c. Quantitative assessment of changes in surface particulate matter concentrations and precursor emissions over China during the COVID-19 pandemic and their implications for Chinese economic activity. Atmos. Chem. Phys. 21 (13), 10065–10080. https://doi.org/10.5194/acp-21-10065-2021.

Koo, B., Wilson, G.M., Morris, R.E., Dunker, A.M., Yarwood, G., 2009. Comparison of Source Apportionment and Sensitivity Analysis in a Particulate Matter Air Quality Model. Environ. Sci. Technol. 43 (17), 6669–6675. https://doi.org/10.1021/es9008129.

Kumar, N., Park, R.J., Jeong, J.I., Woo, J.-H., Kim, Y., Johnson, J., Yarwood, G., Kang, S., Chun, S., Knipping, E., 2021. Contributions of International Sources to PM2.5 in South Korea. Atmos. Environ. 118542. https://doi.org/10.1016/j.atmosenv.2021.118542.

Kurokawa, J., Ohara, T., 2020. Long-term historical trends in air pollutant emissions in Asia: Regional Emission inventory in ASia (REAS) version 3. Atmos. Chem. Phys. 20 (21), 12761–12793. https://doi.org/10.5194/acp-20-12761-2020.

Lorente, A., Folkert Boersma, K., Yu, H., Dörner, S., Hilboll, A., Richter, A., Liu, M., Lamsal, L.N., Barkley, M., De Smedt, I., Van Roozendael, M., Wang, Y., Wagner, T., Beirle, S., Lin, J.-T., Krotkov, N., Stammes, P., Wang, P., Eskes, H.J., Krol, M., 2017. Structural uncertainty in air mass factor calculation for NO2 and HCHO satellite retrievals. Atmos. Meas. Tech. 10 (3), 759–782. https://doi.org/10.5194/amt-10-759-2017.

LTP. 2019. Summary report of the 4th stage (2013–2017) LTP project (Joint research project for long–range transboundary air pollutants in Northeast Asia, issue.

NCEP. (2000) NCEP FNL operational model global tropospheric analyses, continuing from July 1999. 10.5065/D6M043C6.

Oak, Y.J., Park, R.J., Schroeder, J.R., Crawford, J.H., Blake, D.R., Weinheimer, A.J., Woo, J.-H., Kim, S.-W., Yeo, H., Fried, A., Wisthaler, A., Brune, W.H., 2019. Evaluation of simulated O_3 production efficiency during the KORUS-AQ campaign: Implications for anthropogenic NO_x emissions in Korea. Elem Sci Anth 7 (1), 56. https://doi.org/10.1525/elementa.394.

Skamarock, W., Klemp, J., Dudhia, J., Gill, D., Barker, M., Duda, K., Huang, -Y, Wang, W., Powers, J. 2008. A description of the Advanced Research WRF Version 3.

Tan, J., Zhang, Y., Ma, W., Yu, Q., Wang, J., Chen, L., 2015. Impact of spatial resolution on air quality simulation: A case study in a highly industrialized area in Shanghai, China. Atmos. Pollut. Res. 6 (2), 322–333. https://doi.org/10.5094/APR.2015.036.

Uno, I., Wang, Z., Itahashi, S., Yumimoto, K., Yamamura, Y., Yoshino, A., Takami, A., Hayasaki, M., Kim, B.-G., 2020. Paradigm shift in aerosol chemical composition over regions downwind of China. Sci. Rep. 10 (1), 6450. https://doi.org/10.1038/s41598-020-63592-6.

Wang, J., Xu, J., He, Y., Chen, Y., Meng, F., 2016a. Long range transport of nitrate in the low atmosphere over Northeast Asia. Atmos. Environ. 144, 315–324. https://doi.org/10.1016/j.atmosenv.2016.08.084.

Wang, L., Liu, Z., Sun, Y., Ji, D., Wang, Y., 2015. Long-range transport and regional sources of PM2.5 in Beijing based on long-term observations from 2005 to 2010. Atmos. Res. 15737–15748. https://doi.org/10.1016/j.atmosres.2014.12.003.

Wang, Y., Wang, J., Xu, X., Henze, D.K., Wang, Y., Qu, Z., 2016b. A new approach for monthly updates of anthropogenic sulfur dioxide emissions from space: Application to China and implications for air quality forecasts: Top-Down Monthly SO2 Emission Estimate. Geophys. Res. Lett. 43 (18), 9931–9938. https://doi.org/10.1080/16742834.2017.1315631.

Wei, Y., Li, J., Wang, Z.-F., Chen, H.-S., Wu, Q.-Z., Li, J.-J., Wang, Y.-L., Wang, W., 2017. Trends of surface PM2.5 over Beijing–Tianjin–Hebei in 2013–2015 and their causes: emission controls vs. meteorological conditions. Atmos. Oceanic Sci. Lett. 10 (4), 276–283.

Woo, J.-H., Kim, Y., Kim, H.-K., Choi, K.-C., Eum, J.-H., Lee, J.-B., Lim, J.-H., Kim, J., Seong, M., 2020. Development of the CREATE Inventory in Support of Integrated Climate and Air Quality Modeling for Asia. Sustainability 12 (19), 7930. https://doi.org/10.3390/su12197930.

Woo, J.-H., Kim, Y., Kim, J., Park, M., Jang, Y., Kim, J., Bu, C., Lee, Y., Park, R., Oak, Y., Fried, A., Simpson, I., Emmons, L., Crawford, J. (n.d) KORUS Emissions: A comprehensive Asian emissions information in support of the NASA/NIER KORUS-AQ mission. Elementa: Science of the Anthropocene, in press.

Yim, S.H.L., Gu, Y., Shapiro, M.A., Stephens, B., 2019. Air quality and acid deposition impacts of local emissions and transboundary air pollution in Japan and South Korea. Atmos. Chem. Phys. 19 (20), 13309–13323. https://doi.org/10.5194/acp-19-13309-2019.

Zhang, Q., Zheng, Y., Tong, D., Shao, M., Wang, S., Zhang, Y., Xu, X., Wang, J., He, H., Liu, W., Ding, Y., Lei, Y., Li, J., Wang, Z., Zhang, X., Wang, Y., Cheng, J., Liu, Y., Shi, Q., Yan, L., Geng, G., Hong, C., Li, M., Liu, F., Zheng, B., Cao, J., Ding, A., Gao, J., Fu, Q., Huo, J., Liu, B., Liu, Z., Yang, F., He, K., Hao, J., 2019. Drivers of improved PM2.5 air quality in China. Proc. Natl. Acad. Sci. 116 (49), 24463–24469. https://doi.org/10.1073/pnas.1907956116 from 2013 to 2017.

Zhang, Y., Mathur, R., Bash, J.O., Hogrefe, C., Xing, J., Roselle, S.J., 2018. Long-term trends in total inorganic nitrogen and sulfur deposition in the US from 1990 to 2010. Atmos. Chem. Phys. 18 (12), 9091–9106. https://doi.org/10.5194/acp-18-9091-2018.

Zheng, B., Tong, D., Li, M., Liu, F., Hong, C., Geng, G., Li, H., Li, X., Peng, L., Qi, J., Yan, L., Zhang, Y., Zhao, H., Zheng, Y., He, K., Zhang, Q., 2018. Trends in China's anthropogenic emissions since 2010 as the consequence of clean air actions. Atmos. Chem. Phys. 18 (19), 14095–14111. https://doi.org/10.5194/acp-18-14095-2018.